Bulletin of Electrical Engineering and Informatics
Vol. 13, No. 2, April 2024, pp. 734~744
ISSN: 2302-9285, DOI: 10.11591/eei.v13i2.5849

Comparative analysis and validation of advanced control modules for standalone renewable micro grid with droop controller

Savitri Swathi[1], Bhaskaruni Suresh Kumar[2], Jalla Upendar[1]
[1]Department of Electrical Engineering, University College of Engineering, Osmania University, Hyderabad, India
[2]Department of Electrical and Electronics, C.B.I.T, Osmania University, Hyderabad, India

Article Info

Article history:

Received Jan 24, 2023
Revised Aug 16, 2023
Accepted Dec 20, 2023

Keywords:

Adaptive neuro-fuzzy inference system
Fuzzy inference system
Proportional integral derivative
Synchronous reference frame
MATLAB/Simulink

ABSTRACT

A micro grid system with renewable source operation control is a complex part as each source operates at different parameters. This renewable micro grid with multiple sources like solar plants, wind farm, fuel cell, battery backup has to be operated in both grid connected and standalone condition. During grid connection the micro grid, inverter has to inject power to the grid and compensate load in synchronization to the grid voltages. And during standalone condition the inverter is controlled with droop control module which stabilizes the voltage and frequency of the system even during grid disconnection. The droop control module is further updated with new advanced controllers like fuzzy inference system (FIS) and adaptive neuro-fuzzy inference system (ANFIS) replacing the traditional proportional integral derivative (PID) and proportional integral (PI) controllers improving the response rate and for achieving better stabilization. This paper has comparative analysis of the micro grid system with different droop controllers under various operating conditions. Parameters like voltage magnitude (V_{mag}), frequency (F), load and inverter powers (P_{load} and P_{inv}) of the test system are compared with different controllers. A numeric comparison table is given to determine the optimal controller for the inverter operation. The analysis is carried out in MATLAB/Simulink software with graphical and parametric validations.

This is an open access article under the CC BY-SA license.

Corresponding Author:

Savitri Swathi
Department of Electrical Engineering, University College of Engineering, Osmania University
Hyderabad, India
Email: eee.swathi48@gmail.com

1. INTRODUCTION

Micro grid systems (MGS) in today's technological advancements are very efficient and robust to the disturbances and sudden variations of load. These MGS are becoming an integral part of main grid system sharing a very huge power to the grid. In the MGS many small or large sources can be included which can accumulate the power and compensate the load. These MGS sources can be renewable or non-renewable, but due to the present day scenario of climatic disasters due to global warming [1] it is preferable to have renewable sources MGS. These renewable sources can be wind farms, fuel cell plants, photovoltaic (PV) plants, tidal energy, and biogas plants, which produce power from available natural sources like blowing wind, tidal waves, biomass, and solar irradiation [2].

As per the source these modules do not reproduce any hazardous gases or residue which causes pollution and hence they are considered as green energy sources. The power from these source can be

extracted which can be shared to the loads and also can be injected to grid [3]. However the power produced from these sources are capricious as the availability of the natural sources is unpredictable. There are many researches done for maximum and optimal power extraction from these sources with stabilized voltages. As per previous researches considering optimization of the control modules in power electronic converters makes the source more stable and operates at maximum power extraction.

There is also a major hurdle of making these sources operate in standalone conditions as these sources are not much recommendable for individual operation because of their unpredictable power generation [4], [5]. All the sources need to be connected to common power sharing point at a DC bus as DC reduces the complexity for control. The common DC bus needs to be connected with a heavy rating inverter which has the capability of converting the huge DC power to AC power. The DC bus voltage stabilization is very crucial as it has to be maintained at specific value even during wide range of natural parameters variations. The control of the inverter is also very vital as the operation of the inverter has to be synchronized to the grid [6], [7] and also must be operated in standalone condition. The test system with renewable sources connection to the grid through 3-ph inverter can be shown in Figure 1.

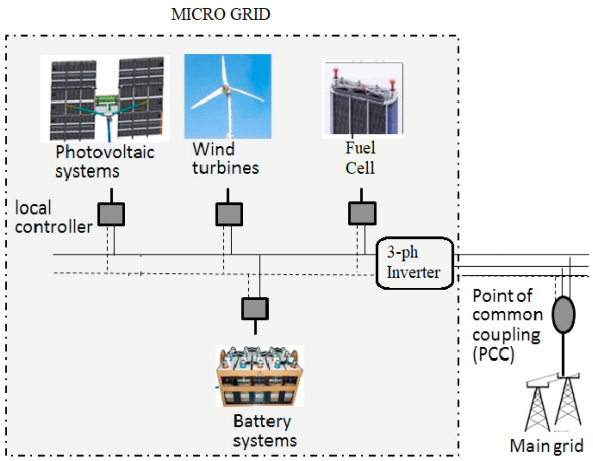

Figure 1. Micro grid test system with renewable sources

In section 1 of this paper the introduction to the test system with selected renewable sources for the analysis are discussed. The configuration of the renewable modules micro grid system with internal stabilizing converters modeling is given in section 2. The control modules for the 3-ph inverter operating in both grid connection and standalone modes are also included in section 2. The section 3 has configuration of droop control module update with fuzzy inference system (FIS) and adaptive neuro-fuzzy inference system (ANFIS) controllers replacing conventional proportional integral derivative (PID) controller. The comparative analysis and graphical validations with results generated by different controllers using Simulink tool is done is section 4. The final section 5 the conclusion to this paper is given with parametric value comparison table between PID, FIS and ANFIS droop controllers determining best controller, followed by references used in this paper.

2. SYSTEM CONFIGURATION

As per the test system introduced in section 1 Figure 1, the renewable source micro grid is integrated with three renewable sources solar plant, fuel cell plant, and wind farm. Along with these renewable sources a battery backup module [8] is also included which supports the renewable micro grid. In the given test system the primary priority renewable sources are wind farm and solar plant from which the complete power is extracted and is either consumed by load, or injected to grid or stored in battery backup module [9].

There are two possible operating conditions; i) grid connected condition-where the loads are compensated by solar, wind plants and grid if needed. In this condition during excess power generation by the renewable sources it is injected to grid after compensating the load and ii) standalone condition-where the grid is not available for the support of the load, therefore the renewable micro grid need to compensate the load [10], [11]. Therefore a battery backup module is activated in the micro grid which supports the load during deficit renewable power conditions. The same battery backup module stores power from the

renewable source during excess generation due to abundant availability of natural sources (solar and wind) [12]. In standalone mode when the battery backup module also fails due to lower state of charge or any other internal failure, another backup renewable source fuel cell is activated [13]. The fuel cell supports the load during battery backup module failure. The test system internal circuit configuration is shown in Figure 2.

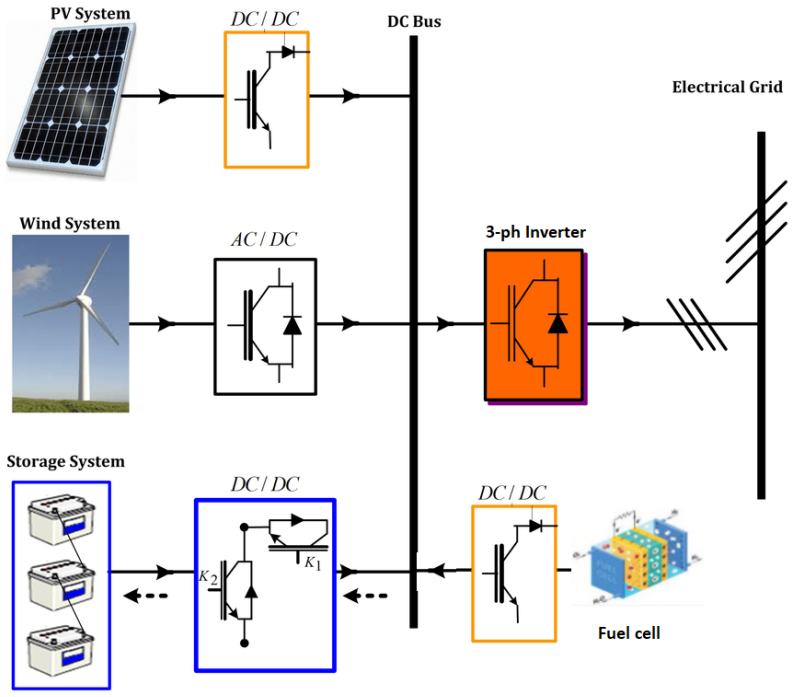

Figure 2. Circuit configuration of renewable micro grid system

As per the given configuration the PV source and fuel cell are connected to booster converter which boosts the source voltages. The boost converter also stabilizes the voltage at specific magnitude even during variable input voltage conditions. The boost converter switch of the PV source is switched by maximum power point tracking (MPPT) module which takes feedback from the PV source current and voltage. A modified P&O MPPT module [14] is adopted to control the duty cycle of the boost switch making the converter to extract maximum power from the source and also maintaining the voltage magnitude at specific value. On the other hand, the fuel cell boost converter switch is controlled by constant voltage oriented controller which generates duty cycle for the switch. The measured output voltage is compared to a reference voltage value generating voltage error [15]. The voltage error is converted to duty cycle by PID controller with tuned Kp and Ki values. The reference voltage of the converter is set as per the system requirement for injection of power to AC side.

The wind farm is permanent magnet synchronous generator (PMSG) connected to a 3-ph rectifier converting AC voltage of the PMSG to DC. The rippled DC is stabilized by buck-boost converter where the switch of the converter is controlled by power signal feedback control MPPT [16]. This MPPT module takes feedback from PMSG rotor speed for generation of reference power. From the reference power the duty cycle for the switch is calculated by torque calculation and PI controller. The buck-boost converter extracts maximum power from the machine as per the available wind speed. The battery backup module is integrated to a two switch bidirectional converter which can charge and discharge the battery as per the given conditions. The battery backup module is activated with respect to availability of 3-ph grid. An islanding detection algorithm [17] with voltage magnitude, frequency and power exchange parameters of the 3-ph grid are considered for the activation of battery backup module. As per these parameters given threshold ranges the triggering of the battery backup module breaker is done. The circuit breaker is turned ON when the detection parameters are not in given range indicating grid failure or disconnection condition creating micro grid standalone mode. The fuel cell source [18] is activated when the battery backup module fails to compensate the load during standalone mode due to low state of charge or battery fault.

All these renewable and backup sources are connected to a common DC link where a 3-ph inverter is interconnected between the 3-ph grid and DC link. The 3-ph inverter is controlled by two different control structures which are selected as per the grid availability. During grid connection the inverter is operated with synchronous reference frame (SRF) control structure [19] which makes the inverter to operate in synchronization to the grid voltages. The SRF control module is a conventional controller which takes inputs of the inverter currents, DC link voltage and voltages of the grid. Many researches are done on this controller where multiple DC sources are interconnected to grid with reduced harmonics. During standalone mode a novel droop control module is switched in for controlling the inverter. The switching between the controllers is done by the islanding detection algorithm which was used for the battery backup module.

The droop controller [20] controls the inverter so as to make it operate with stabilized AC voltage and frequency injecting the renewable power to the load. The conventional droop control module with voltage and frequency control can be observed in Figure 3. As per Figure 3 the voltage (V) and angular frequency (ω) PID controllers are replaced with FIS or ANFIS controllers for faster and reduced disturbance operation of the control module [21]. This makes the inverter to operate more stable with reduced response rate and reduced ripple in the voltages. As per the new controllers the load power compensation is accurately achieved and the frequency oscillations are also reduced. The configuration of the FIS and ANFIS controllers for the voltage and frequency regulators are done in next section.

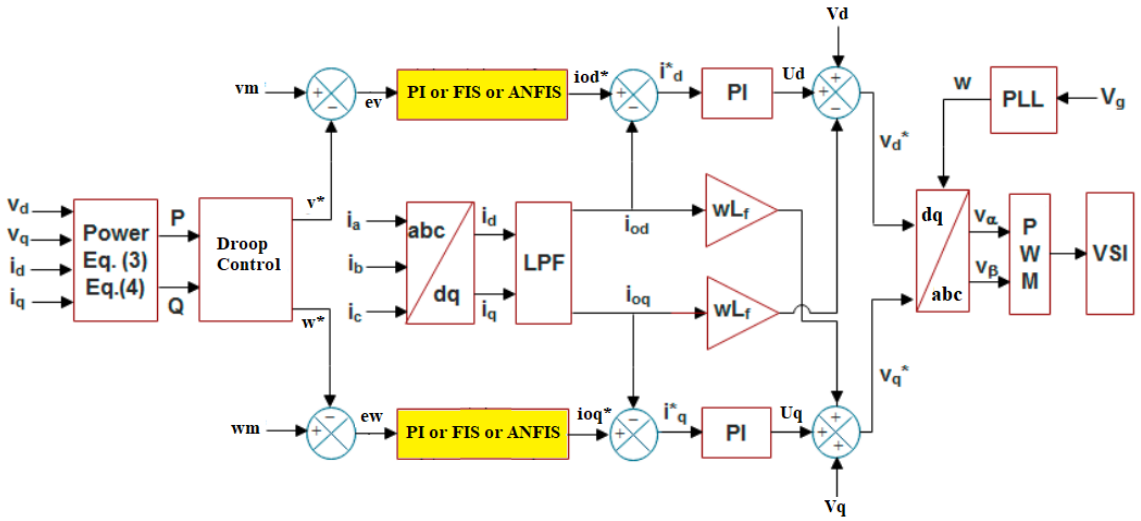

Figure 3. Droop control module with different controllers

3. CONTROLLER MODULES

As per the droop control module [22] in Figure 3 the reference current components iod* and ioq* are generated by the current regulators. With a PID controller in the regular place the current expression are given as (1) and (2):

$$i_{od}^{*} = (v^{*} - v_{m})(K_{p} + \int K_{i} \, . \, dt) \quad (1)$$

$$i_{oq}^{*} = (w^{*} - w_{m})(K_{p} + \int K_{i} \, . \, dt) \quad (2)$$

The Kp and Ki are the proportional and integral gains which are tuned as per the response time. Here v_m and w_m are the measured voltage magnitude on the AC side and frequency of the inverter. The v^* and w^* are the reference voltage magnitude and frequency generated by the droop control with inputs taken from active and reactive power (P&Q) of the inverter. The reference parameters v^* and w^* with respect to P&Q are given as (3) and (4):

$$v^{*} = v_{n} - k_{v}Q \quad (3)$$

$$w^{*} = w_{n} - k_{w}P \quad (4)$$

In the given expressions (3) and (4) v_n and w_n are the fundamental voltage and frequency taken as 1 pu and 314 rad/sec. The k_v and k_w are the voltage and frequency constants expressed as (5) and (6):

$$k_v = \frac{v_{max} - v_{min}}{Q_{max}} \quad (5)$$

$$k_w = \frac{w_{max} - w_{min}}{P_{max}} \quad (6)$$

where $v_{max}\ and\ v_{min}$ are the maximum and minimum permitted voltages taken as 1.05 and 0.95 respectively. $w_{max}\ and\ w_{min}$ are the maximum and minimum permitted frequency taken as 317 and 310. P_{max} and Q_{max} are the maximum injected active and reactive powers given as per the availability of renewable power. In (1) and (2) are updated replacing PID with FIS and ANFIS controller improving the iod* and ioq* signals response and reducing oscillations. This improves the droop controller performance [23] where the impact is observed on reference controlling signals vd* and vq*.

3.1. FIS control module

The FIS control module is advancement to the conventional PID controller where the output response is a bit faster and also with reduced disturbances. This makes the FIS controller [24] to operate the droop controller with faster response to the changes in the grid system. The FIS controller needs two inputs which are denoted as error 'E' and change in error 'CE'. The E signal is the comparison of either voltage or frequency parameters as per (1) and (2). The CE is generated by comparison of the present value of E considered as E(k) and previous value of E considered as E(k-1) expressed as (7):

$$CE = E(k) - E(k-1) \quad (7)$$

The FIS structure considered is 'mamadani' where the membership functions are set in specific range as per the input parameters. The output of the FIS control modules will either be iod* or ioq* as per the given input 'ev' or 'ew' respectively [25]. The input and output membership functions are shown in Figure 4.

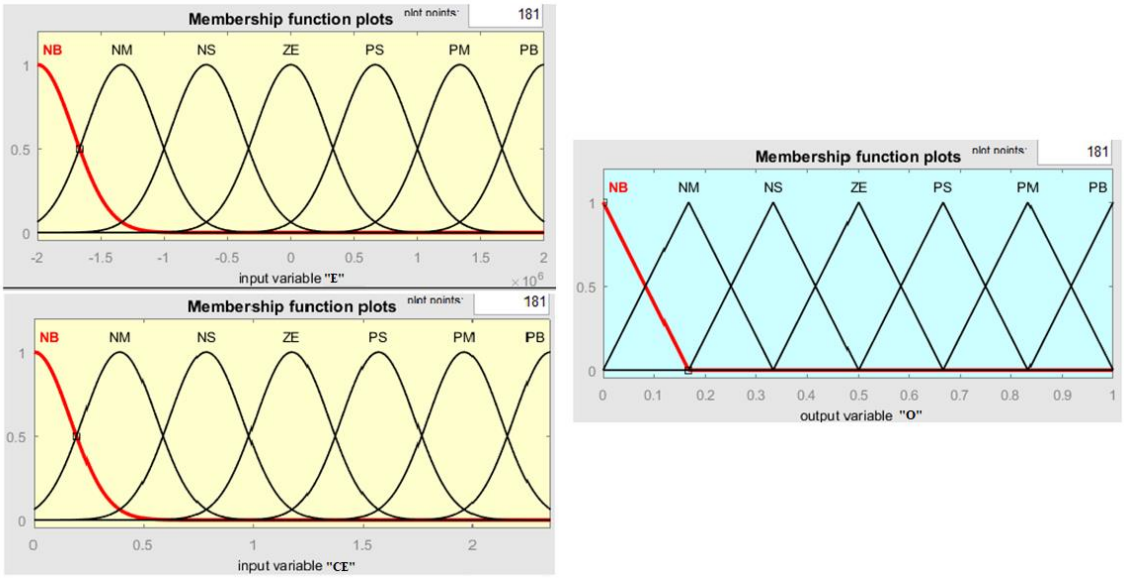

Figure 4. Membership functions of E, CE and O variables in FIS control module

The names of the functions are defined as; PB is positive big, PM is positive medium, PS is positive small, ZE is zero, NB is negative big, NM is negative medium, and NS is negative small. The 'E' range in set between -100 and 100, 'CE' range is set between -1 to 1 and the output 'O' range is set between -50 to 50. The input functions are gauss type and output functions are triangular type. These types are taken for faster converging of the output variable. As per the given 7 functions in each parameter, the rule base is given in Table 1. As per given rule table the FIS controllers of voltage and frequency regulators generate iod* and ioq* in the specific given ranges.

Table 1. FIS rule base

ce / e	NB	NM	NS	ZE	PS	PM	PB
NB	NB	NB	NB	NB	NM	NS	ZE
NM	NB	NB	NB	NM	NS	ZE	PS
NS	NB	NB	NM	NS	ZE	PS	PM
ZE	NB	NM	NS	ZE	PS	PM	PB
PS	NM	NS	ZE	PS	PM	PB	PB
PM	NS	Z	PS	PM	PB	PB	PB
PB	Z	PS	PM	PB	PB	PB	PB
NB	NB	NB	NB	NB	NM	NS	ZE

3.2. ANFIS control module

For further improvement of the droop control structure the FIS module is replaced with ANFIS control module [26] which is more advanced to the conventional fuzzy control. The conventional fuzzy functions are trained and tuned further using optimization algorithm for more fast response rate and reduced disturbances. The structure considered for ANFIS control is 'Sugeno' where the input functions type will be same as FIS (gauss) but the output parameter type will be set to 'constant' with the same range of FIS. The input signal is only 'E' which is the either voltage or frequency error. The Figure 5 are the output functions in the ANFIS control module.

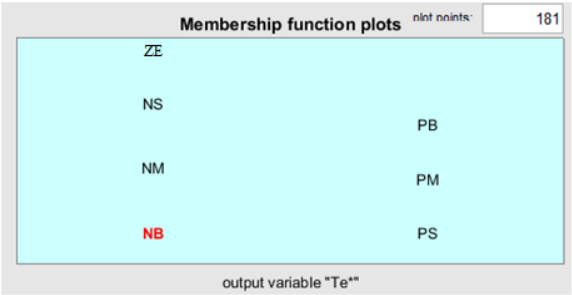

Figure 5. Output parameter with constant functions

These input and output functions are trained from the data taken from input and output of conventional PID controller. The data is imported into the ANFIS tool for training the functions using 'back-propagation' optimization algorithm [27]. The new trained data and previous data can be seen in Figure 6.

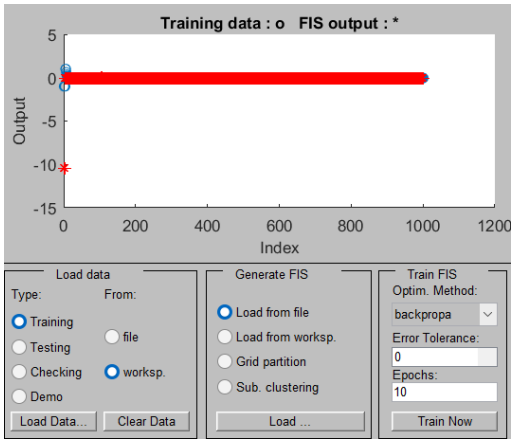

Figure 6. ANFIS training from PID data

With the new trained data the input parameter functions are updated as shown in Figure 7. The updated Sugeno functions of both voltage and frequency regulators are inserted replacing FIS controller and a comparative analysis is done [28]. The analysis includes different measuring signals of the micro grid parameters with PI, PID, FIS and ANFIS controller updated in droop control module during standalone operating mode. The results are compared and validated in further sections.

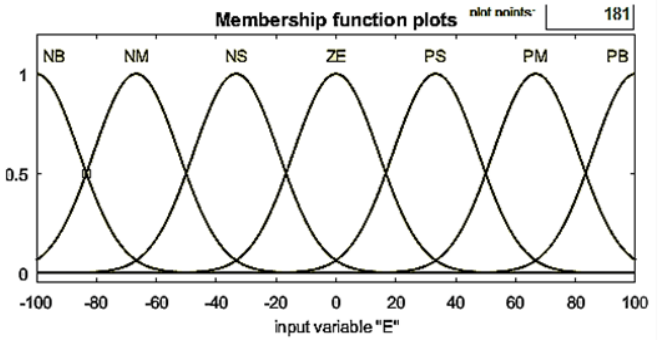

Figure 7. New ANFIS trained input parameter 'E'

4. SIMULATION RESULTS

As per the given configuration of each source and control modules for extraction of power from these source the modeling of the complete grid system with renewable sources is done in Simulink. Each renewable source has it is own individual control for maximum power injection to the grid or load. The battery backup module is activated with islanding detection algorithm which also switches the control of the inverter between SRF to droop control. The 3-ph inverter droop control in standalone mode is updated with different controllers (FIS and ANFIS) and the simulation is run with different operating conditions. The modeling of the test system with the given source modules and grid system can be seen in Figure 8.

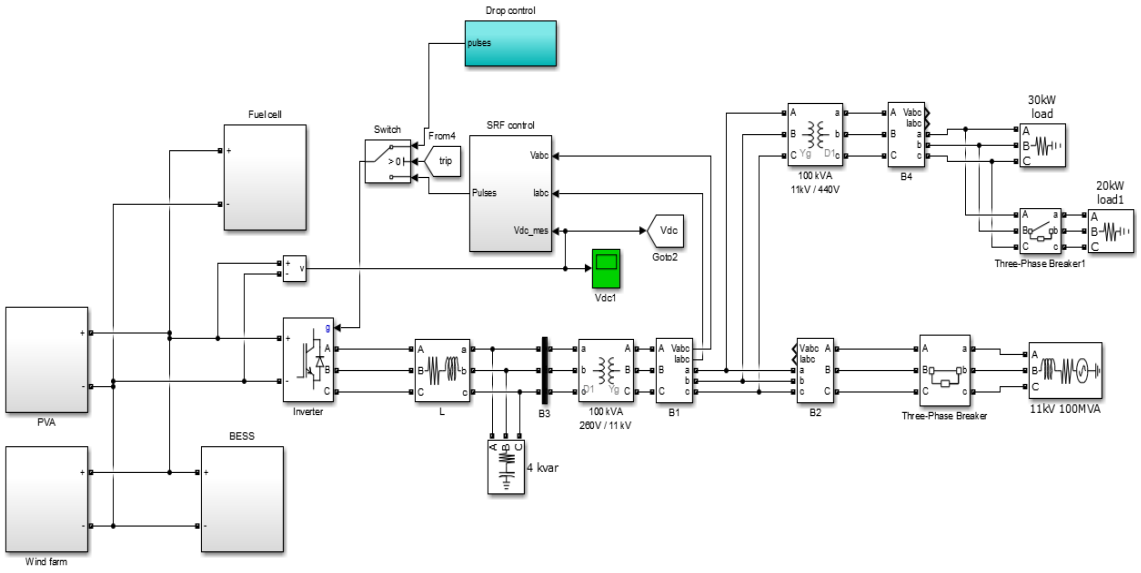

Figure 8. Test system modeling

The total simulation time is considered to be 5 sec where the grid is connected until 0.5 sec. After grid disconnection at 0.5 sec the battery backup module is activated by trigging ON the circuit breaker of the battery module. At 1.2 sec the solar irradiation is dropped to 500 W/mt^2 from 1,000 W/mt^2, at 2 sec the load is increased from 30 to 50 kW. At 3.5 sec the battery module is failed and disconnected, activating the fuel

cell source replacing the battery. The battery compensation power is replaced by the fuel cell source which is the final backup to the micro grid. The parameter configuration of the complete grid is given in Table 2.

Table 2. System configuration parameters

Name of the parameter	Values
Grid rating	11 kV 50 Hz 100 MVA
Load parameters	L1–30 kW, L2–20 kW
PV module	V_{mp}=54.7 V, I_{mp}=5.58 A, V_{oc}=64.2 V, I_{sc}=5.96 A, N_p=10, N_s=5. $P_{pv\ total}$=15 kW,
	Boost converter–L_b=1 mH, C_{in}=100 µF, C_{out}=12 mF.
Wind farm module	PMSG–67N-mt, 560 Vdc, 1,700 rpm
	Turbine–12 kW, Base wind speed=12 m/s, base rotational speed=1.2 pu
	Boost converter–L_b=100 µH, C_{in}=1,000 µF, C_{out}=1,000 µF
BESS module	Lithium-Ion V_{nom}=250 V, Capacity=100 Ah
	Bidirectional converter-L_b=161.95 µH, C_{out}=220 µF
Fuel cell module	V_{nom}=300 V, I_{nom}=133.3 A, V_{end}=220 V, I_{end}=225 A.
	Boost converter–Lb=1 mH, Cin=100 µF, Cout=12 mF.
VSI LC filter	L_f=250 mH, C_f=2.6 kVAR
Islanding detection limits	0.88<V_{mag}<1.1, -1>Q>1, 49.3<f<50.5
SRF controller gains	DC voltage gains-K_p=7, K_i=800
	Current controller gains–K_p=0.3, K_i=20
Droop controller gains	V & w controller gains–K_p=0.05, K_i=0.01
	Current controller gains–K_p=0.3, K_i=20

As per the given system parameters and the operating conditions in total simulation time of 5 sec the results of each module are present in Figure 9. All the graphs are generated with different controllers (PI, PID, FIS and ANFIS) in the droop control modules with comparisons done in the same graph with respect to time.

Figure 9 is a comparison of the DC bus voltage between all controllers. This voltage is set at 500 V reference as per the voltage requirement on the AC side. As per the graphical comparison the DC bus voltage with ANFIS controller is more stable and reduced ripple. The value is also near to 500 V as that of FIS controller. The lower peak generation during battery failure at 3.5 sec is also eliminated. The Figure 10 is the PV source power extraction comparison between conventional P&O and modified P&O MPPT.

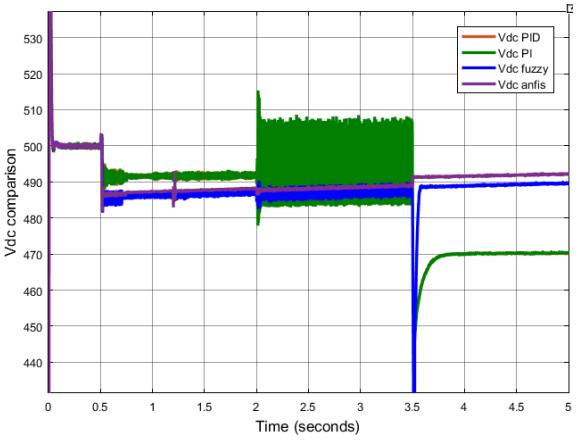

Figure 9. DC bus voltage comparison

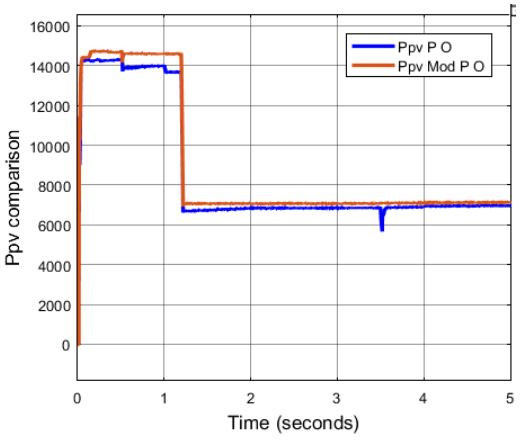

Figure 10. PV source injected power comparison

As per the comparison in Figure 10 of the PV power (Ppv) the modified MPPT control is more stable and settles faster. The power extraction is also increased by 500 W during the initial state with solar irradiation 1,000 W/mt^2. In Figure 11 the magnitudes of inverter 3-ph AC voltage comparisons are taken which determine the ANFIS controller advantage. The new controller eliminates the upper and lower peak value generations during battery failure maintaining the voltage near to 1 pu in any operating condition.

As the voltage peaks are eliminated the peaks of power injection by micro grid are also eliminated which can be observed in Figure 12. Figure 13 is the frequency evaluation of the point of common coupling (PCC) voltages. As seen in Figure 13 the frequency with ANFIS controller is more stable and with lower peak value generations during changing operating conditions. As the micro grid power is stabilized with

lower ripple and peak generations the load power is also stable and is compensated as per the requirement shown in Figure 14. The final validations and parametric comparisons of different measurements are noted in Table 3 considering different variables of the graphs Figures 13 and 14.

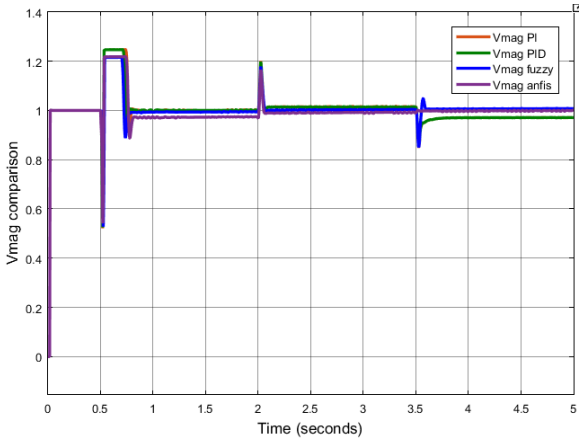

Figure 11. Inverter 3-ph voltage magnitude comparison

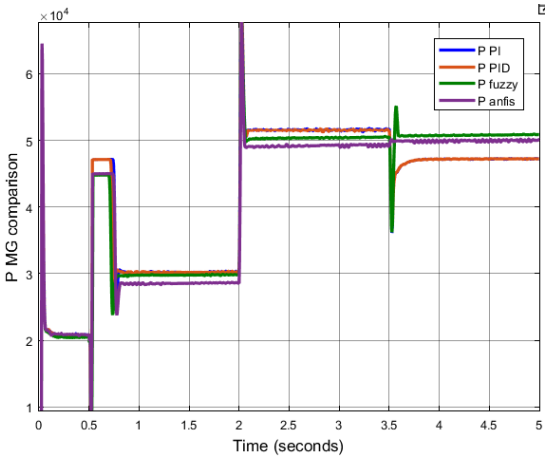

Figure 12. Total micro-grid power injection comparison

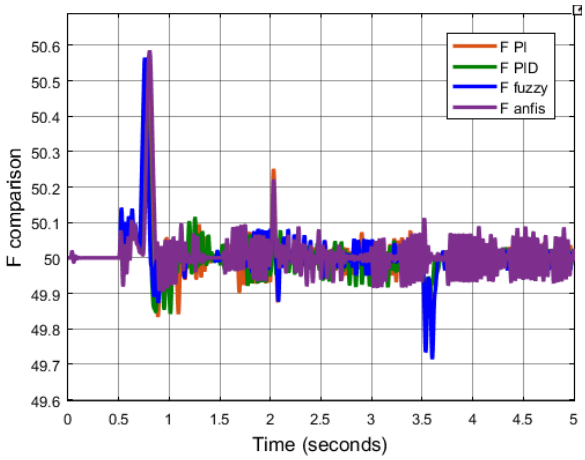

Figure 13. PCC frequency comparison

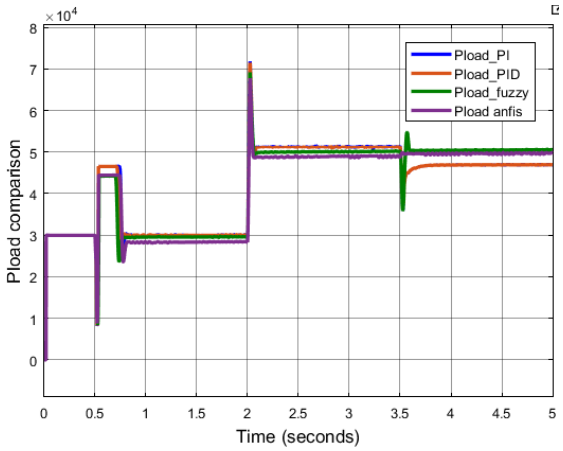

Figure 14. Total load power comparison

Table 3. Comparative analysis

Name of the parameter	PI	PID	FIS	ANFIS
P-MG (kW)	46	46	50	50
Vdc ripple (%)	4.92	4.92	0.81	0.52
Vdc magnitude (V)	470	470	490	492
Vpcc magnitude (pu)	1.05	0.97	0.97	0.99
F settling time (sec)	0.9	0.9	0.5	0.3
F ripple (%)	0.5	0.2	0.2	0.15

5. CONCLUSION

The implementation of the complete grid system with renewable micro grid in achieved. The system is tended to operate in different operating modes which include grid connected mode, standalone mode, battery support mode, battery failure mode. A comparative analysis is carried out on the system operated with all these modes and different parameters are compared by changing the controllers. The voltages and powers at specific locations are compared when the micro grid is operated in standalone mode where the 3ph inverter is operated by droop controller. As per the given parametric comparison the ANFIS controller is considered

to be a best choice for generating the current references in the droop controller. With reduced ripple and oscillations in the current signals the inverter operates more stable and the grid parameters are improved. The ANFIS droop controllers has lower ripple and faster settling times for any changes in the grid. Therefore, this control module is determined to be optimum for the operation of the micro grid inverter.

REFERENCES

[1] M. Z. A. Khan, "Causes and consequences of greenhouse effect and its catastrophic problems for earth," *International Journal of Sustainability Management and Information Technologies*, vol. 3, no. 4, 2017, doi: 10.11648/j.ijsmit.20170304.11.

[2] X. Ma, S. Liu, H. Liu, and S. Zhao, "The selection of optimal structure for stand-alone micro-grid based on modeling and optimization of distributed generators," *IEEE Access*, vol. 10, pp. 40642–40660, 2022, doi: 10.1109/ACCESS.2022.3164514.

[3] B. J. Abdulelah, Y. I. M. Al-Mashhadany, S. Algburi, and G. Ulutagay, "Modeling and analysis: Power injection model approach for high performance of electrical distribution networks," *Bulletin of Electrical Engineering and Informatics*, vol. 10, no. 6, pp. 2943–2952, Dec. 2021, doi: 10.11591/eei.v10i6.3126.

[4] C. Zhang, Y. Xu, and Z. Y. Dong, "Robustly coordinated operation of a multi-energy micro-grid in grid-connected and islanded modes under uncertainties," *IEEE Transactions on Sustainable Energy*, vol. 11, no. 2, pp. 640–651, Apr. 2020, doi: 10.1109/TSTE.2019.2900082.

[5] M. Haseeb, S. A. A. Kazmi, M. M. Malik, S. Ali, S. B. A. Bukhari, and D. R. Shin, "Multi objective based framework for energy management of smart micro-grid," *IEEE Access*, vol. 8, pp. 220302–220319, 2020, doi: 10.1109/ACCESS.2020.3041473.

[6] J. A. A. Silva, J. C. López, N. B. Arias, M. J. Rider, and L. C. P. da Silva, "An optimal stochastic energy management system for resilient microgrids," *Applied Energy*, vol. 300, Oct. 2021, doi: 10.1016/j.apenergy.2021.117435.

[7] P. Wang, W. Wang, and D. Xu, "Optimal sizing of distributed generations in DC microgrids with comprehensive consideration of system operation modes and operation targets," *IEEE Access*, vol. 6, pp. 31129–31140, 2018, doi: 10.1109/ACCESS.2018.2842119.

[8] N. Mezzai, S. Belaid, D. Rekioua, and T. Rekioua, "Optimization, design and control of a photovoltaic/wind turbine/battery system in Mediterranean climate conditions," *Bulletin of Electrical Engineering and Informatics*, vol. 11, no. 5, pp. 2938–2948, Oct. 2022, doi: 10.11591/eei.v11i5.3872.

[9] A. Das and Z. Ni, "A computationally efficient optimization approach for battery systems in islanded microgrid," *IEEE Transactions on Smart Grid*, vol. 9, no. 6, pp. 6489–6499, Nov. 2018, doi: 10.1109/TSG.2017.2713947.

[10] A. M. Ferrario *et al.*, "A model-based parametric and optimal sizing of a battery/hydrogen storage of a real hybrid microgrid supplying a residential load: Towards island operation," *Advances in Applied Energy*, vol. 3, Aug. 2021, doi: 10.1016/j.adapen.2021.100048.

[11] C. Wang, Y. Liu, X. Li, L. Guo, L. Qiao, and H. Lu, "Energy management system for stand-alone diesel-wind-biomass microgrid with energy storage system," *Energy*, vol. 97, pp. 90–104, Feb. 2016, doi: 10.1016/j.energy.2015.12.099.

[12] S. K. Bilgundi, H. Pradeepa, A. Kadam, and L. M. Venkatesh, "Energy management schemes for distributed energy resources connected to power grid," *Indonesian Journal of Electrical Engineering and Computer Science*, vol. 28, no. 1, pp. 30–40, Oct. 2022, doi: 10.11591/ijeecs.v28.i1.pp30-40.

[13] M. N. Hamidi, D. Ishak, M. A. A. M. Zainuri, C. A. Ooi, and T. Tarmizi, "Asymmetrical multi-level DC-link inverter for PV energy system with perturb and observe based voltage regulator and capacitor compensator," *Journal of Modern Power Systems and Clean Energy*, vol. 9, no. 1, pp. 199–209, 2021, doi: 10.35833/MPCE.2019.000147.

[14] X. Tong, C. Hu, C. Zheng, T. Rui, B. Wang, and W. Shen, "Energy market management for distribution network with a multi-microgrid system: A dynamic game approach," *Applied Sciences (Switzerland)*, vol. 9, no. 24, Dec. 2019, doi: 10.3390/app9245436.

[15] V. V. S. N. Murty and A. Kumar, "Multi-objective energy management in microgrids with hybrid energy sources and battery energy storage systems," *Protection and Control of Modern Power Systems*, vol. 5, no. 1, Jan. 2020, doi: 10.1186/s41601-019-0147-z.

[16] Y. Wang *et al.*, "Energy management of smart micro-grid with response loads and distributed generation considering demand response," *Journal of Cleaner Production*, vol. 197, pp. 1069–1083, Oct. 2018, doi: 10.1016/j.jclepro.2018.06.271.

[17] M. Marzband, S. S. Ghazimirsaeid, H. Uppal, and T. Fernando, "A real-time evaluation of energy management systems for smart hybrid home Microgrids," *Electric Power Systems Research*, vol. 143, pp. 624–633, Feb. 2017, doi: 10.1016/j.epsr.2016.10.054.

[18] M. R. B. Khan, J. Pasupuleti, J. Al-Fattah, and M. Tahmasebi, "Optimal grid-connected PV system for a campus microgrid," *Indonesian Journal of Electrical Engineering and Computer Science*, vol. 12, no. 3, pp. 899–906, Dec. 2018, doi: 10.11591/ijeecs.v12.i3.pp899-906.

[19] A. Ahmad *et al.*, "An optimized home energy management system with integrated renewable energy and storage resources," *Energies*, vol. 10, no. 4, Apr. 2017, doi: 10.3390/en10040549.

[20] M. M. Zadeh, Z. Afshar, M. J. Harandi, and S. M. T. Bathaee, "Frequency control of low inertia microgids in presence of wind and solar units using fuzzy-neural controllers," in *2022 26th International Electrical Power Distribution Conference, EPDC 2022*, May 2022, pp. 54–59, doi: 10.1109/EPDC56235.2022.9817192.

[21] T. A. Jumani, M. W. Mustafa, M. M. Rasid, N. H. Mirjat, Z. H. Leghari, and M. Salman Saeed, "Optimal voltage and frequency control of an islanded microgrid using grasshopper optimization algorithm," *Energies*, vol. 11, no. 11, Nov. 2018, doi: 10.3390/en11113191.

[22] K. Rouzbehi, A. Miranian, J. I. Candela, A. Luna, and P. Rodriguez, "A generalized voltage droop strategy for control of multiterminal DC grids," *IEEE Transactions on Industry Applications*, vol. 51, no. 1, pp. 607–618, Jan. 2015, doi: 10.1109/TIA.2014.2332814.

[23] O. Feddaoui, R. Toufouti, and L. Djamel, "Active and reactive power sharing in micro grid using droop control," *International Journal of Electrical and Computer Engineering*, vol. 10, no. 3, pp. 2235–2244, Jun. 2020, doi: 10.11591/ijece.v10i3.pp2235-2244.

[24] X. Chen, L. Wang, H. Sun, and Y. Chen, "Fuzzy logic based adaptive droop control in multiterminal HVDC for wind power integration," *IEEE Transactions on Energy Conversion*, vol. 32, no. 3, pp. 1200–1208, Sep. 2017, doi: 10.1109/TEC.2017.2697967.

[25] R. Thangella, S. R. Yarlagadda, and J. Sanam, "Optimal design for solar cell and fuel cell renewable source to enhance the power quality in a micro grid system," Jul. 2022, doi: 10.1109/ICICCSP53532.2022.9862356.

[26] N. Mahmud, A. Zahedi, and A. Mahmud, "A cooperative operation of novel PV inverter control scheme and storage energy management system based on ANFIS for voltage regulation of grid-tied PV system," *IEEE Transactions on Industrial Informatics*, vol. 13, no. 5, pp. 2657–2668, Oct. 2017, doi: 10.1109/TII.2017.2651111.

[27] P. García, C. A. García, L. M. Fernández, F. Llorens, and F. Jurado, "ANFIS-Based control of a grid-connected hybrid system integrating renewable energies, hydrogen and batteries," *IEEE Transactions on Industrial Informatics*, vol. 10, no. 2, pp. 1107–1117, May 2014, doi: 10.1109/TII.2013.2290069.
[28] D. C. Sekhar, P. V. V. R. Rao, and R. Kiranmayi, "A novel efficient adaptive-neuro fuzzy interfaced system control based smart grid to enhance power quality," *International Journal of Electrical and Computer Engineering*, vol. 12, no. 4, pp. 3375–3387, Aug. 2022, doi: 10.11591/ijece.v12i4.pp3375-3387.

BIOGRAPHIES OF AUTHORS

Savitri Swathi is a research scholar at the Department of Electrical Engineering University College of Engineering, Osmania University. She is working as an Assistant Professor in the Institute of Aeronautical Engineering College Since 2012 in Dundigal, Hyderabad. She guided 2 PG and 4 UG projects, her research areas are power systems, power quality, and power electronics. She can be contacted at email: eee.swathi48@gmail.com.

Bhaskaruni Suresh Kumar is an Associate Professor at the Electrical and Electronics Engineering Department at Chaitanya Bharathi Institute of Technology, Osmania University. He holds a Ph.D. degree in power quality-power systems in the year 2014 from JNTU Kukatpally, Hyderabad, Telangana. His research areas are power systems and power quality. He can be contacted at email: bskbus@gmail.com.

Jalla Upendar is an Assistant Professor Electrical Engineering Department at the University College of Engineering, Osmania University. He holds a Ph.D. degree in intelligent Approach for fault classification of power transmission systems with a specialization in Electrical Engineering in the Indian Institute of Technology (IIT), Roorkee, Uttarakhand, India in 2010. His research areas are power systems, power electronics, FACTS devices, and artificial intelligent techniques. He can be contacted at email: dr.8500003210@gmail.com.